Molecular Biology of the Cell
Vol. 12, 2453–2468, August 2001

Targeting of Shiga Toxin B-Subunit to Retrograde Transport Route in Association with Detergent-resistant Membranes

Thomas Falguières,* Frédéric Mallard,* Carole Baron,* Daniel Hanau,† Clifford Lingwood,‡ Bruno Goud,* Jean Salamero,* and Ludger Johannes*§

*Unité Mixte de Recherche 144 Institut Curie/ Centre National de la Recherche Scientifique, F-75248 Paris Cedex 05, France;† Institut National de la Santé et de la Recherche Médicale E99-08, F-67065 Strasbourg Cedex, France; and ‡Hospital for Sick Children, Toronto M5G 1X8, Canada

Submitted October 17, 2000; Revised March 27, 2001; Accepted May 30, 2001
Monitoring Editor: Howard Riezman

In HeLa cells, Shiga toxin B-subunit is transported from the plasma membrane to the endoplasmic reticulum, via early endosomes and the Golgi apparatus, circumventing the late endocytic pathway. We describe here that in cells derived from human monocytes, i.e., macrophages and dendritic cells, the B-subunit was internalized in a receptor-dependent manner, but retrograde transport to the biosynthetic/secretory pathway did not occur and part of the internalized protein was degraded in lysosomes. These differences correlated with the observation that the B-subunit associated with Triton X-100-resistant membranes in HeLa cells, but not in monocyte-derived cells, suggesting that retrograde targeting to the biosynthetic/secretory pathway required association with specialized microdomains of biological membranes. In agreement with this hypothesis we found that in HeLa cells, the B-subunit resisted extraction by Triton X-100 until its arrival in the target compartments of the retrograde pathway, i.e., the Golgi apparatus and the endoplasmic reticulum. Furthermore, destabilization of Triton X-100-resistant membranes by cholesterol extraction potently inhibited B-subunit transport from early endosomes to the *trans*-Golgi network, whereas under the same conditions, recycling of transferrin was not affected. Our data thus provide first evidence for a role of lipid asymmetry in membrane sorting at the interface between early endosomes and the *trans*-Golgi network.

INTRODUCTION

Shiga toxin and the closely related verotoxins (VTs), produced by *Shigella dysenteriae* and enterohemorrhagic strains of *Escherichia coli*, respectively, are bacterial protein toxins composed of two subunits, A and B (Sandvig and van Deurs, 1996). The A-subunit is the actual toxin whose rRNA *N*-glycosidase activity leads to the inhibition of protein biosynthesis in target cells. For cellular binding and intracellular transport, the A-subunit depends on its noncovalent interaction with the B-subunit (STxB) composed of a homopentamer of B-fragments. STxB binds to the cellular toxin receptors: the glycolipid Gb_3 for Shiga toxin, VT1, VT2, and VT2c; and Gb_4 for VT2e (Lingwood, 1993). A close correlation exists between infection with VT-producing *E. coli* and outbreaks of enterohemorrhagic colitis and hemolytic and uremic syndrome, whereas Shiga toxin has been related to vascular damage during shigellosis (reviewed in O'Brien *et al.*, 1992).

In a number of cell lines, Shiga toxin or STxB alone can be detected in the endoplasmic reticulum (ER) (Sandvig *et al.*, 1992, 1994; Khine and Lingwood, 1994; Johannes *et al.*, 1997) from where the A-subunit is thought to pass into the cytosol (Hazes and Read, 1997; Simpson *et al.*, 1999; Wesche *et al.*, 1999). The intracellular transport pathway allowing the toxin access to the ER has recently been studied in detail. After internalization into EE of HeLa cells, the protein appears to be transported directly to the Golgi apparatus, bypassing late endosomes (Mallard *et al.*, 1998), thus describ-

§ Corresponding author. E-mail address: johannes@curie.fr.

Abbreviations used: Bafi, bafilomycin; DC, dendritic cell; Dex3, 3-kD dextran; Dex2000, 2000-kD dextran; DRM, detergent-resistant membrane; EE, early endosomes; EEA1, early endosomal antigen 1; ER, endoplasmic reticulum; FACS, fluorescence-activated cell sorting; Gb_3, globotriaosylceramide; imDC, immature dendritic cell; LPS, lipopolysaccharide; mDC, mature dendritic cell; mβCD, methyl-β-cyclodextrin; MHC, major histocompatibility complex; PPMP, 1-phenyl-2-hexadecanoyl-amino-3-morpholino-1-propanol; SLO, streptolysin O; STxB, Shiga toxin B-subunit; TCA, trichloroacetic acid; Tf, transferrin; TfR, transferrin receptor; TGN, *trans*-Golgi network; TLC, thin-layer chromatography; VT, verotoxin.

ing a new pathway that may also be used by endogenous proteins such as TGN38 (Ghosh *et al.*, 1998). Furthermore, passage from the Golgi apparatus to the ER also appears to occur via a novel transport route that is independent of classical retrograde transport markers, such as the KDEL-receptor and coatomer protein I, but dependent on Rab6 function (Johannes *et al.*, 1997; Girod *et al.*, 1999; White *et al.*, 1999).

In contrast to HeLa cells, mouse macrophages, human primary monocytes, and monocyte cell lines are resistant to the inhibitory activity of Shiga toxin on protein biosynthesis despite the expression of Gb_3 (Tesh *et al.*, 1994; Ramegowda and Tesh, 1996; van Setten *et al.*, 1996). Interest has recently been focused on monocyte-derived cells, especially DCs, due to their unique capacity to induce primary and secondary immune responses (reviewed in Banchereau and Steinman, 1998; Mellman *et al.*, 1998). This feature is both the result of and depends on a tight regulation of multiple characteristics, such as the expression levels of MHC class I, class II, and costimulatory molecules; migration to lymphoid organs; and antigen internalization and degradation. Our data indicate that STxB can introduce exogenous antigenic peptides into the endogenous MHC class I-restricted antigen presentation pathway of these cells (Lee *et al.*, 1998; Haicheur *et al.*, 2000).

We have here studied STxB traffic in monocyte-derived macrophages and DCs. Because the Shiga toxin receptor is a glycosphingolipid, we have paid special attention to STxB association with detergent-resistant membranes (DRMs). DRMs, which have been given different names such as microdomains, lipid rafts, and detergent-insoluble glycolipid-enriched domains (Hooper, 1999), are in fact preferentially composed of (glyco)sphingolipids, saturated glycerophospholipids, and cholesterol, and recent evidence suggests that they exist as microdomains in biological membranes (Friedrichson and Kurzchalia, 1998; Harder *et al.*, 1998; Varma and Mayor, 1998). They have been ascribed functions in intracellular transport and in signal transduction: in polarized cells, glycosyl phosphatidyl inositol-anchored proteins are targeted to the apical surface through their association with lipid rafts (Brown and Rose, 1992; reviewed in Simons and Ikonen, 1997); membrane-associated signaling molecules and receptors are often recovered from DRMs, and it has been suggested that such topological restriction could favor signal transduction by bringing enzymes and receptor complexes in proximity (Hakomori *et al.*, 1998). Two views have been proposed to explain the formation of DRMs, either via an interaction between glycosphingolipid headgroups (Simons and Ikonen, 1997) or between lipid acyl chains (Brown and London, 1998).

We have found that STxB was targeted to the retrograde transport pathway and associated with DRMs in HeLa cells, but not in monocyte-derived cells, suggesting a functional correlation between both phenomena. In agreement with this hypothesis we observed that in HeLa cells, STxB was resistant to Triton X-100 extraction all along its retrograde transport, and that the destabilization of DRMs by cellular cholesterol extraction led to an inhibition of STxB transfer from EE to the TGN. Our data thus provide first evidence for a role of lateral lipid asymmetry in membrane sorting in the retrograde transport route.

MATERIALS AND METHODS

Cells and Cell Culture

Human monocytes were obtained from blood of healthy donors with their prior consent according to published procedures (Faradji *et al.*, 1994) with the use of continuous flow centrifugation leukapheresis and counterflow centrifugation. Macrophages were derived from these monocytes by colony stimulating factor-1 (Genetics Institute, Cambridge, MA) treatment at 1000 U/ml for 6–8 d in complete RPMI 1640 medium supplemented with 2 mM L-glutamine, 1% sodium pyruvate, 1% nonessential amino acids, and 10% heat-inactivated fetal calf serum (Life Technologies, Paisley, United Kingdom). Ninety-six percent of the cells were macrophages, as judged from their strong adherence to plastic dishes, their morphology, their nonspecific esterase activity (α-naphtyl esterase kit from Sigma, L'Isle d'Abeau Chesnes, France), and their high level expression of CD14. These macrophages expressed low levels of MHC class II molecules, CD1a, c-fms, and no CD83 at their plasma membrane, as determined by fluorescence-activated cell sorting (FACS) analysis. Immature dendritic cells (imDCs) were derived from primary monocytes in the presence of 50 ng/ml granulocyte/monocyte-colony stimulating factor (Novartis, Rueil-Malmaison, France) and 1000 U/ml interleukin-4 (Schering-Plough, Dardilly, France). ImDCs were differentiated in mature dendritic cells (mDCs) by additional treatment for 1–2 d with 30 ng/ml tumor necrosis factor-α (Genzyme, Cambridge, MA), as published (Sallusto *et al.*, 1995). ImDCs expressed MHC class II molecules, CD1a, and c-fms at their plasma membrane, but no CD83 or CD14. In mDCs that had typical dendrite morphology, c-fms cell surface expression was down-regulated and MHC class II, CD83, and CD86 cell surface expression was up-regulated. All experiments that are described in this manuscript were performed at least twice on cells obtained from different donors.

HeLa cells (Johannes *et al.*, 1997) and primary skin fibroblasts (Dimon-Gadal *et al.*, 1998) were cultured as published.

Antibodies and Other Reagents

The antibodies used for the FACS characterization of the above-described cells have been described elsewhere (Baron *et al.*, 2001). The monoclonal and polyclonal anti-STxB antibodies were obtained as described previously (Johannes *et al.*, 1997; Mallard *et al.*, 1998). The Fab-fragment of 13C4 was prepared according to the manufacturer's instructions with the use of a commercial kit (Pierce, Rockford, IL). Polyclonal anti-TGN46 antibody was provided by R. Pepperkok (European Molecular Biology Laboratories, Heidelberg, Germany) and the mouse monoclonal anti-transferrin receptor (TfR) antibody H68.4 by I. Trowbridge (The Salk Institute, San Diego, CA). Polyclonal anti-B23 antibody (Santa Cruz Biotechnology, Santa Cruz, CA), secondary fluorophore-coupled $F(ab')_2$ (Jackson Immunresearch, West Grove, PA), 3-kDa dextran (Dex3) and 2000-kDa dextran (Dex2000) (Molecular Probes, Eugene, OR), lipopolysaccharide (LPS), methyl-β-cyclodextrin (mβCD) (Sigma), and 1-phenyl-2-hexadecanoyl-amino-3-morpholino-1-propanol (PPMP) (Calbiochem, La Jolla, CA) were obtained from the indicated commercial sources.

FACS Analysis

For cell surface FACS analysis, cells were resuspended in phosphate-buffered saline (PBS) containing 3% fetal calf serum and 0.1% sodium azide (resuspension buffer), incubated for 30 min on ice with STxB, and washed three times in cold resuspension buffer. Cells were then incubated for 30 min at 4°C with 13C4 monoclonal antibody (mAb), washed three times with cold resuspension buffer, and incubated with a fluorescein isothiocyanate-coupled anti-mouse $F(ab')_2$. Cell-associated fluorescence was quantified with an FACS spectrofluorimeter (Becton Dickinson, San Jose, CA). Staining with isotype control antibodies was performed in parallel. For in-

ternal FACS analysis, 0.1 μM STxB (5 μg/ml) associated or not with the 13C4-derived Fab fragment (see below) was incubated for 30 min at 37°C with macrophages. The cells were then put on ice, washed, fixed for 10 min with 3% paraformaldehyde, quenched, permeabilized with the use of 0.05% saponin, and stained as described above. The background obtained with isotypic control antibody was subtracted.

Glycolipid and Cholesterol Extraction Procedures and Overlay

Lipid extraction was done according to the method of Bligh and Dyer (1959). The indicated numbers of cells in 1 ml of aqueous buffer were injected into 3.75 ml of chloroform/methanol (1:2). After mixing, 1.25 ml of chloroform and 1.25 ml of water were added. Phases were separated after mixing, and the hydro-alcoholic phase was washed once with 1.5 ml of chloroform. In a preliminary experiment, the hydro-alcoholic phase was shown not to contain Gb_3. The combined chloroform phases were dried under nitrogen, and lipids were saponified at 56°C for 1 h in 1 ml of methanol/KOH. The saponification reaction was once again extracted as described above, and the chloroform phase was washed once with methanol/water (1:1). The isolated neutral glycolipids were spotted on high-performance thin-layer chromatography (TLC) plates (Merck, Darmstadt, Germany) and separated with chloroform/methanol/water (65:25:4). Dried plates were soaked in 0.1% polyisobutylmethacrylate in hexane, floated for 1 h in blocking solution, followed by incubation with STxB (20 nM), primary polyclonal anti-STxB, and secondary horseradish peroxidase, or alkaline phosphatase-coupled anti rabbit antibodies. Reactive bands were revealed with the use of enhanced chemiluminescence or chemifluorescence (Amersham Pharmacia Biotech, Little Chalfont, United Kingdom) and PhosphorImager. Free cellular cholesterol was determined as published (Gamble *et al.*, 1978) after lipid extraction (Bligh and Dyer, 1959) without saponification. For cholesterol back-addition experiments, 40 mg of cholesterol was coated on the walls of a glass vial, 5 ml of 20 mM mβCD in transport buffer was added and incubated after sonication for 15 h at 37°C. The resulting solution was filtered and added at the indicated concentrations to cells.

DRM Preparation and Analysis

DRMs were prepared as published (Benting *et al.*, 1999). Briefly, the required amount of cells for 300 μg of total protein was washed once with PBS and resuspended in 0.2 ml of 2× TNE (1× TNE: 25 mM Tris/HCl pH 7.4, 150 mM NaCl, 2.5 mM EDTA, a mixture of protease inhibitors containing phenylmethylsulfonyl fluoride, leupeptin, chymostatin, pepstatin, antipain, and aprotinin). All steps were performed on ice. Then 0.2 ml of 2% Triton X-100 solution was added, the mixture was incubated for 30 min on ice, and Optiprep (Sigma) was added to a final concentration of 40%. The solution was overlaid with 2.3 and 0.8 ml of 30 and 5% Optiprep in TNE, respectively, and spun at 4°C, 28,000 rpm for 4 h (SW41 rotor; Beckman Instruments, Palo Alto, CA). The gradient was fractionated from the top. DRMs were found at the 5/30% interface. To analyze the fractions, Western blotting and dot blot analysis were done according to standard procedures. To determine the effect of cholesterol extraction with mβCD on DRM stability (Figure 10B), postnuclear supernatant containing 300 μg of protein was incubated for 30 min at 37°C in the absence or presence of 2.5, 5, or 10 mM mβCD. The solution was replaced on ice, and Triton X-100 was added to 1% final concentration. DRMs were then purified as described above.

Immunofluorescence Methods

Immunofluorescence was performed as previously described (Mallard *et al.*, 1998). Briefly, cells were fixed at room temperature for 10 min in 3% paraformaldehyde, quenched with ammonium chloride, permeabilized with 0.05% saponin, incubated with the indicated primary or secondary antibodies, mounted, and viewed by confocal microscopy (Leica Microsystems, Mannheim, Germany). Dex3 and Dex2000 were added continuously at 0.5 mg/ml. Bafilomycin (Bafi; Fluka, L'Isle d'Abeau Chesnes, France) and ammonium chloride were added to cells at the indicated concentrations 30 min before STxB, and were then present throughout the experiment.

For Fab binding studies, STxB and Fab-fragment were mixed for 30 min on ice at the indicated molar ratios. The mixtures were then added to cells for 30 min at 37°C, upon which the cells were washed, fixed, and stained with Fab-fragment and the indicated primary and secondary antibodies. For Triton X-100 extraction on living cells, the cells were put on ice, washed once with PBS containing 1 mM $MgCl_2$ and 0.5 mM $CaCl_2$, and incubated for 1 min in 1% Triton/PIPES buffer (80 mM PIPES, pH 6.8, 5 mM EGTA, 1 mM $MgCl_2$). The buffer was then removed and 3% paraformaldehyde was added for 15 min at room temperature.

Biochemistry and Internalization Assay

Trichloroacetic acid (TCA) precipitation experiments, sulfation analysis, STxB iodination to specific activities of 5000 cpm/ng, Scatchard analysis, and glycosylation analysis were done as described previously (Johannes *et al.*, 1997; Mallard *et al.*, 1998). To determine endogenous sulfation, sulfated proteins in supernatants obtained after quantitative STxB immunoprecipitation were precipitated with 10% TCA, retained on GF/C glass fiber filters (Whatman, Maidstone, United Kingdom), and counted. For Scatchard analysis, residual binding after addition of a 100-fold excess of nonlabeled competitor protein was deduced from the obtained values.

To measure STxB internalization, a recently developed assay was used (Johannes, Pezzo, Mallard, Tenza, Wiltz, Benichou, Erdtmann, Antony, and Benaroch, unpublished data). In short, a STxB mutant with three C-terminal lysines, termed STxB-K_3, was produced and coupled to NHS-SS-biotin (Pierce). Biotinylated STxB-K_3 was bound to HeLa cells on ice and then internalized for the indicated times at 37°C. Subsequent treatment with 100 mM of the membrane impermeable reducing agent sodium 2-mercaptoethanesulfonic acid (MESNA) on ice for 16 min led to cleavage of >80% of the biotin on cell surface exposed STxB-K_3 (Figure 9A, 4°C), whereas biotin on internal STxB-K_3 was protected. After lysis in RIPA buffer and immunoprecipitation with the anti-STxB mAb, samples were loaded on Tris-Tricine gels, and probed after transfer with streptavidin-alkaline phosphatase (Jackson Immunoresearch). Band intensities were quantified with the use of a PhosphorImager. The percentage of internalized STxB corresponds to the signal obtained on the +MESNA sample (internalized) divided by the signal obtained on the −MESNA sample (total cell associated).

Retrograde Transport Assay and Transferrin (Tf) Recycling on Permeabilized Cells

The details on the retrograde transport assay will be published elsewhere (Mallard, Tang, Galli, Antony, Yue, Tenza, Goud, Hong, Johannes, unpublished data). In brief, STxB-$Sulf_2$ was internalized for 45 min at 19.5°C into sulfate-starved HeLa cells (Mallard *et al.*, 1998). Streptolysin (SLO) was then bound to these cells on ice for 10 min, followed by washings on ice. Then the cells were incubated for 10 min at 37°C for permeabilization, and 15 min at 37°C in the absence or presence of mβCD at the indicated concentrations (Figure 10, C–E). Alternatively, 10 mM mβCD was added at 37°C for 10 min right from permeabilization on, and followed by a 10-min incubation at 37°C in the presence of the indicated doses of cholesterol saturated mβCD (Figure 10F). The incubation solutions were replaced by buffer containing 3 mg/ml HeLa cell cytosol, ATP-regeneration system and radioactive sulfate, followed by incubation at 37°C for 30 min, and STxB immunoprecipitation after cell lysis in RIPA buffer. Sulfated STxB was quantified after gel electrophoresis and autoradiography with the use of PhosphorImager (Mallard *et*

al., 1998). The sulfation of endogenous proteins and proteoglycans was determined in parallel by TCA-precipitation from immunoprecipitation supernatants.

For Tf recycling, 0.12 μCi/ml iodinated Tf (PerkinElmer Life Science Products, Boston, MA) were incubated with HeLa cells at 19.5°C, as described above. After SLO permeabilization and cholesterol extraction, recycling was determined for 30 min at 37°C in the absence or presence of cytosol and/or energy, as indicated. Part of recycling was found to be cytosol independent, as previously published (Galli *et al.*, 1994; Advani *et al.*, 1999), and recycling that depended on cytosol was also energy-dependent.

RESULTS

Characterization of STxB Internalization Pathway in Macrophages and DCs

We first determined whether in addition to human primary monocytes (van Setten *et al.*, 1996), monocyte-derived macrophages, and DCs also expressed the glycosphingolipid Gb_3 (CD77), which has been identified as the Shiga toxin receptor (Lingwood *et al.*, 1987). In particular, DCs were chosen for this study because of their central role in the induction of primary and secondary immune responses (Peters *et al.*, 1996; Hart, 1997; Mellman *et al.*, 1998), making them preferred targets for immunotherapeutic approaches to treatment of cancer and infectious diseases. To evaluate expression of the receptor, neutral glycolipids were extracted from human peripheral blood monocytes, monocyte-derived macrophages and imDCs (Sallusto and Lanzavecchia, 1994), and HeLa cells, followed by TLC analysis. With the use of an overlay technique, Gb_3 was detected (Figure 1A) and quantified (Table 1) by PhosphorImager. Gb_3 expression was comparable between different monocyte-derived cells and ~20-fold lower than in HeLa cells (Table 1).

In agreement with the reduced level of Gb_3 expression, macrophages, imDCs, and mDC-bound small amounts of STxB on ice, as visualized by immunofluorescence microscopy (our unpublished results) or FACS (Figure 1B, gray shaded areas). Quantification by Scatchard analysis of STxB binding to macrophages showed that cell association was saturable, and that these cells bound 4×10^5 molecules/cell with a K_D of 85 nM (Table 1). Addition of a 100-fold excess of nonlabeled competitor STxB over iodinated STxB resulted in a significant inhibition of radiolabeled protein binding. HeLa cells had 4×10^7 binding sites per cell, and the K_D was 19 nM. The apparent difference in affinity is likely to be a result of the lower Gb_3 density in monocytes or macrophages, making cooperative binding less efficient. However, when macrophages or imDCs were incubated for 30 min with 5 μg/ml (0.1 μM) of fluorophore-coupled STxB at 37°C, significant cellular labeling could be detected (Figure 1B, solid black lines). Labeling in imDCs was heterogeneous, as noted before for other cell types (Sandvig *et al.*, 1994). Internalization into mDCs was inefficient, consistent with the notion that endocytosis is down-modulated in these cells (Garrett *et al.*, 2000).

We next tested whether receptor binding was necessary for STxB internalization into cells derived from peripheral blood monocytes. Attempts to inhibit Gb_3 synthesis in these cells with the ceramide glucosyltransferase inhibitor PPMP failed, most likely because in these nondividing cells, Gb_3 was very stable (our unpublished results). We then used the anti-STxB mAb 13C4, which is a neutralizing antibody for

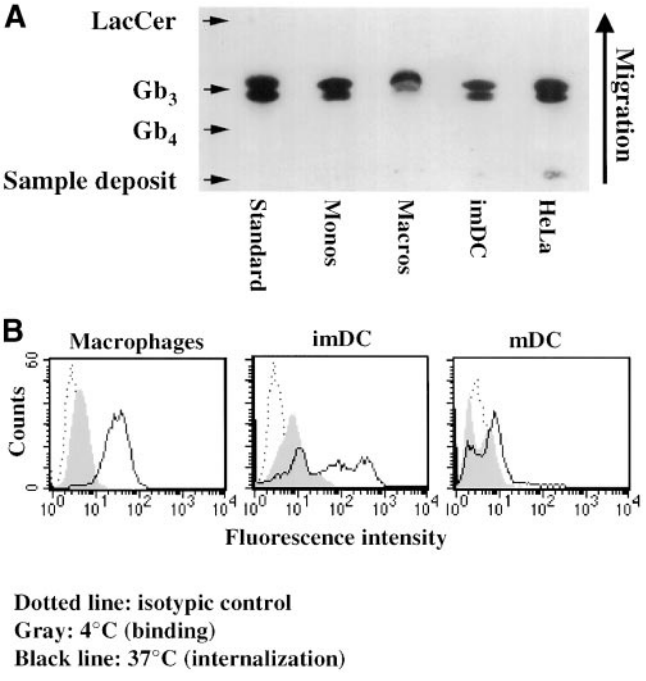

Figure 1. (A) TLC analysis of Gb_3 expression in various cells. Neutral glycolipids were extracted from 1×10^7 monocytes, 2×10^7 macrophages, 2×10^7 imDCs, and 1×10^6 HeLa cells, separated by TLC, and Gb_3 was detected and quantified (Table 1) by overlay with STxB. (B) FACS analysis of STxB binding to and internalization into monocyte-derived cells. Fluorescein-labeled STxB (0.1 μM; 5 μg/ml) was incubated on ice (gray profiles) or for 30 min at 37°C (black lines) with the indicated cells that were then analyzed by FACS. Background signal of nonlabeled cells is also shown (dotted lines). Note the weak but detectable binding after incubation on ice and strong signal after incubation at 37°C.

Shiga toxin (Strockbine *et al.*, 1985), and found that it inhibited STxB binding to Gb_3 (our unpublished results). To avoid immune-complex interaction with high-affinity Fc-receptors on macrophages and dendritic cells, a Fab-fragment of the 13C4 antibody was generated that, when prebound to the STxB, also strongly reduced the STxB–Gb_3 interaction on TLC plates (Figure 2A) or in the plasma membrane of HeLa cells (our unpublished results). This inhibitory activity of the Fab-fragment was paralleled by a reduction of STxB internalization into macrophages after formation of the Fab/STxB complex, as determined by internal FACS (Figure 2B). Immunofluorescence analysis confirmed these data, showing that after prebinding to the Fab-fragment (Figure 2C, +Fab), STxB internalization was reduced compared with STxB internalization in the absence of the Fab-fragment (Figure 2C, −Fab). Importantly, Dex3 entered the cells in the presence of the Fab-fragment showing that the cells retained their overall internalization capacity under these conditions. In the absence of the Fab-fragment, STxB accumulated in punctuate cytoplasmic structures, which most likely were endosomes because they also contained cointernalized Dex3, and in distinct subnuclear domains where the protein colocalized with the nucleolar marker B23 (our unpublished results). Some of the

Table 1. Quantification of STxB retrograde transport and Gb_3 expression

Cell types	Glycosylation (%)	Gb_3 ($\mu g/10^6$ cells)	Binding sites ($\times 10^6$/cell)	K_D (nM)
HeLa	7.3 ± 1.4 (10)	0.94 ± 0.16 (9)	40	19
HeLa + PPMP	6.3 ± 1.7 (7)	0.25 ± 0.05 (5)	1.2 ± 0.6 (4)	19 ± 7 (4)
Macrophages	background	0.04 ± 0.02 (4)	0.4 ± 0.2 (4)	85 ± 30 (4)
Macrophage + LPS	1.1 ± 0.5 (3)	0.27 ± 0.1 (4)	2.8 ± 1.2 (4)	21 ± 3 (4)
Monocytes	background	0.06 ± 0.03 (3)	n.d.	n.d.
Monocytes + LPS	1.5 ± 0.5 (3)	0.27 ± 0.2 (4)	n.d.	n.d.
imDC	background	0.04 (2)	n.d.	n.d.

n.d., not determined.

STxB-Glyc-KDEL was bound to the indicated cells on ice and after washings, the cells were incubated for 4 h at 37°C. Arrival in the ER was quantified through the detection of the protein's glycosylation (percentage of glycosylated, cell-associated protein). Gb_3 was quantified on TLC plates after extraction of neutral glycolipids and detection by overlay. Binding sites and the apparent affinity of STxB-Glyc-KDEL for the indicated cells were determined by Scatchard analysis. Data are given as means ± SEM (number of experiments in parentheses).

Dex3-positive structures contained low amounts of STxB, suggesting that Dex3 used several entry pathways (Figure 2C, −Fab, insets). In summary, these data suggested that STxB entered macrophages and DCs in a receptor-dependent manner, probably in interaction with Gb_3.

As shown in Figure 2C, STxB colocalized with Dex3 when internalized at 37°C. The result was quite different when STxB was internalized for short times at 37°C in the presence of Dex2000 (Figure 3A). Dex2000, due to its size, entered cells by macropinocytosis that occurs constitutively in monocyte-derived macrophages and DCs, and Dex2000 was found in typical large macropinosomes that were observed only after longer times of incubation, however (our unpublished results). Internalization profiles containing Dex2000 accumulated only low levels of STxB (Figure 3A). At 19.5°C, STxB and Dex3 were still endocytosed and colocalized in EE (Figure 3B), whereas the internalization of Dex2000 was strongly reduced (Figure 3C), consistent with the notion that macropinocytosis is highly temperature-dependent (Pratten and Lloyd, 1979). STxB thus entered macrophages in a receptor-dependent manner via micropinocytosis.

STxB Targeting to Late Endosomes/Lysosomes in Macrophages

It was surprising to find an extensive overlap of STxB and Dex3 labeling in macrophages (Figure 2C). This suggested that in contrast to HeLa cells, where the STxB bypasses the late endocytic pathway (Mallard *et al.*, 1998), in macrophages STxB was targeted to late endosomes/lysosomes. Thus, we monitored the degradation of radiolabeled STxB in the endocytic pathway by measuring the appearance of TCA-soluble counts in the external medium. As previously described, only 3% of HeLa cell-associated iodinated STxB became TCA soluble, even after prolonged incubation (Mallard *et al.*, 1998; Figure 4A). The result was quite different in macrophages (Figure 4A) and imDCs (our unpublished results). Up to 55% of cell-associated STxB was degraded after 120 min (Figure 4A). This degradation was inhibited in the presence of drugs that increase endosomal pH, namely, Bafi and ammonium chloride (Figure 4B), consistent with the notion that in macrophages and DCs, STxB was in part delivered to late endosomes/lysosomes.

This hypothesis was further confirmed by immunofluorescence experiments. When internalized at 19.5°C into macrophages, STxB accumulated in EEA1 containing EE (Figure 4C). The cells were then washed, and STxB labeling intensity decreased importantly within minutes of a subsequent shift to 37°C (Figure 4D). When the remaining signal was enhanced, it appeared that STxB could be detected in part in tubular structures that were also labeled for the lysosomal glycoprotein Lamp2 (Figure 4D, insets), suggesting that the protein was transported to late endosomes/lysosomes where it was degraded. Indeed, a shift to 37°C in the presence of Bafi prevented the disappearance of STxB labeling (Figure 4E). The protein accumulated in Lamp2-positive structures that had a vacuolar morphology (Figure 4E), but remained also detectable in EEA1-containing structures (our unpublished results), suggesting that Bafi not only blocked STxB degradation but also slowed STxB transport into the late endocytic pathway (Clague *et al.*, 1994). The persistence of STxB staining in the presence of Bafi furthermore showed that the loss of STxB labeling in the absence of the drug (Figure 4D) was not simply due to recycling of the protein to the external medium. These biochemical and morphological studies thus strongly suggested that in macrophages and monocytes, STxB was in part targeted to late endosomes/lysosomes where it underwent degradation.

STxB Is Targeted to Golgi Apparatus or ER in HeLa Cells, but not in Untreated Monocyte-derived Cells

The other hallmark of STxB traffic in HeLa cells is that the protein has access to the Golgi apparatus and the ER. Thus, it was surprising to note that in macrophages, we detected no obvious juxta-nuclear or reticular STxB accumulation indicative of Golgi or ER staining, respectively (Figure 2C). To test this directly, STxB was incubated with macrophages and imDCs that were then labeled for the TGN marker protein TGN46 (Figure 5A), the medial-Golgi marker CTR433, or the ER marker calnexin (our unpublished results). No significant overlap between these compartment-

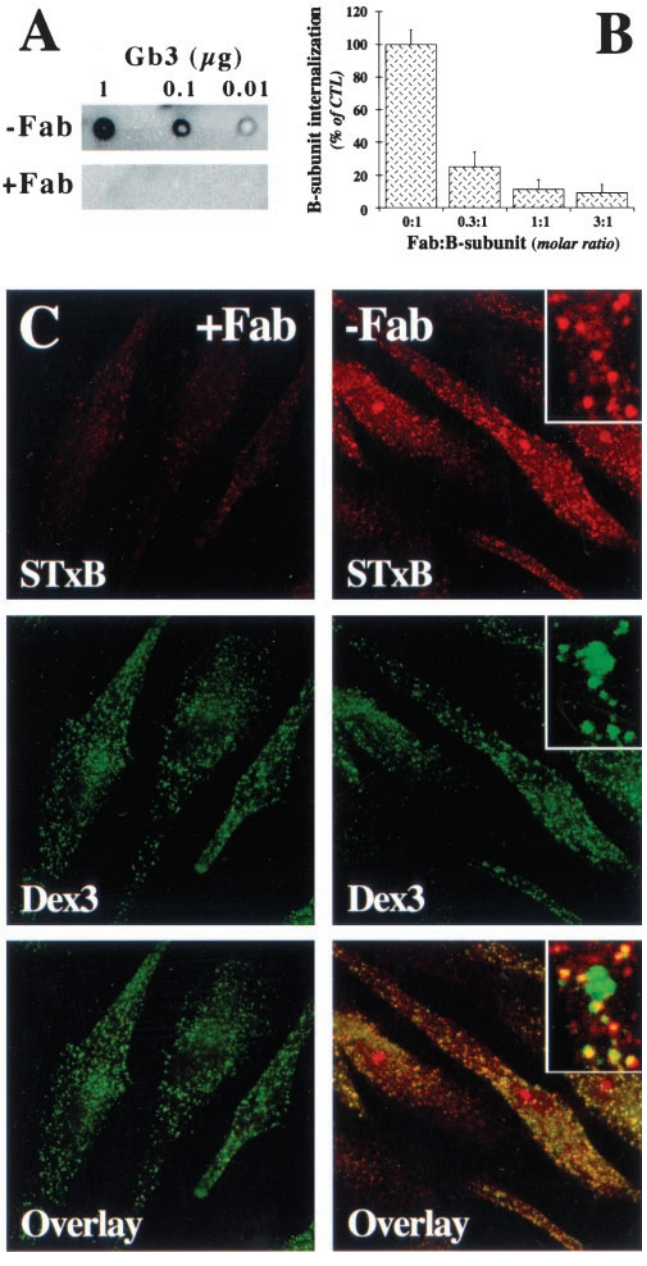

Figure 2. Receptor-dependent STxB internalization into macrophages. (A) Fab-fragment of 13C4 mAb inhibits STxB binding to Gb_3. Gb_3 was spotted on TLC plates that were then incubated with STxB prebound (+Fab) or not (−Fab) to the Fab-fragment of 13C4, followed by detection with the use of the STxB overlay technique. Note that Fab-bound STxB did not interact with Gb_3. (B) FACS analysis of the effect on internalization of STxB prebinding to the Fab-fragment of 13C4. STxB (0.1 μM; 5 μg/ml) was prebound to increasing doses of the Fab-fragment, as indicated. The complex was then incubated with macrophages for 30 min at 37°C. Cells were put on ice, fixed, permeabilized, and incubated with Fab-fragment (to reveal STxB that had not been prebound to the Fab-fragment) and secondary fluorescein-coupled anti-mouse antibody, followed by FACS analysis. Means of three experiments (± SEM) are shown. (C) Immunofluorescence analysis of the effect on internalization of STxB prebinding to the Fab-fragment of 13C4. Experiments as described in B, except that the cells were viewed by indirect immunofluorescence. STxB (0.1 μM; 5 μg/ml) was prebound (+Fab) or not (−Fab) to the Fab-fragment at a molar ration of 1:1 and then cointernalized with fluorescein-coupled Dex3 for 30 min at 37°C into macrophages. Insets show high-magnification views. Note that some Dex3-containing structures contained only low amounts of STxB.

specific markers and STxB was observed. Furthermore, also in the presence of Bafi, no STxB was detected in the Golgi apparatus, indicating that the apparent transport deficiency was not due to a premature degradation of the protein (Figure 4F). We verified that other primary cells could transport STxB into the biosynthetic/secretory pathway, as in HeLa cells. Figure 5A shows that this is the case for primary human skin fibroblasts, in which STxB was targeted to the Golgi apparatus.

We used recently developed modified versions of STxB to obtain quantitative information on its passage into the Golgi apparatus or the ER (Johannes *et al.*, 1997; Johannes and Goud, 1998; Mallard *et al.*, 1998). STxB-Glyc-KDEL and STxB-$Sulf_2$ carry, respectively, an *N*-glycosylation site or a tandem of protein sulfation sites at their C termini, allowing to monitor arrival in the ER via glycosylation by ER-located oligosaccharyl transferase (Johannes *et al.*, 1997), or arrival in the TGN via sulfation by TGN-located sulfotransferase (Johannes *et al.*, 1997; Mallard *et al.*, 1998). Iodinated STxB-Glyc-KDEL was internalized, after prebinding, into HeLa cells or continuously into macrophages. After the indicated times, the cells were lysed and lysates were analyzed by gel electrophoresis and autoradiography. STxB-Glyc-KDEL was glycosylated in HeLa cells (Figure 5B; see arrow for the glycosylation product), whereas even after prolonged incubation, no glycosylation product was found on macrophages (Figure 5B), imDCs, mDCs, or monocytes (our unpublished results). Otherwise, proteolytic cleavage products were detected in both HeLa cells and monocyte-derived cells (Figure 5B, lowest bands). The same results were obtained when STxB-Glyc-KDEL was bound to monocyte-derived cells before internalization (Table 1). To analyze access to the TGN, HeLa cells, macrophages (Figure 5C) or imDCs (our unpublished results) were incubated for the indicated times with STxB-$Sulf_2$ and radioactive sulfate. After immunoprecipitation, radiolabeled STxB-$Sulf_2$ was revealed by autoradiography. As expected, the protein was labeled in HeLa cells (Figure 5C). However, no radiolabel immunoprecipitated with anti-STxB antibody in macrophages (Figure 5C), whereas sulfation obtained on endogenous proteins was comparable in both cell types (our unpublished results).

To assess whether the observed transport differences were solely due to differences in receptor expression levels, HeLa cells were treated for 2 d with the glycosylceramide synthase inhibitor PPMP (Abe *et al.*, 1992) to reduce Gb_3 expression fourfold, and macrophages and monocytes were treated with LPS (van Setten *et al.*, 1996), which resulted in a fivefold increase of Gb_3 expression (Table 1). Through both treatments, similar Gb_3 levels per cell were obtained in all cell types. We furthermore showed that STxB binding to LPS-treated macrophages or PPMP-treated HeLa cells occurred with the same apparent affinity, and that both cell types had similar numbers of binding sites per cell (Table 1). Even under these conditions, however, retrograde transport, as determined by glycosylation analysis (see above), was still five- to sevenfold less efficient in macrophages or monocytes than in HeLa cells (Table 1), suggesting that in addition to receptor expres-

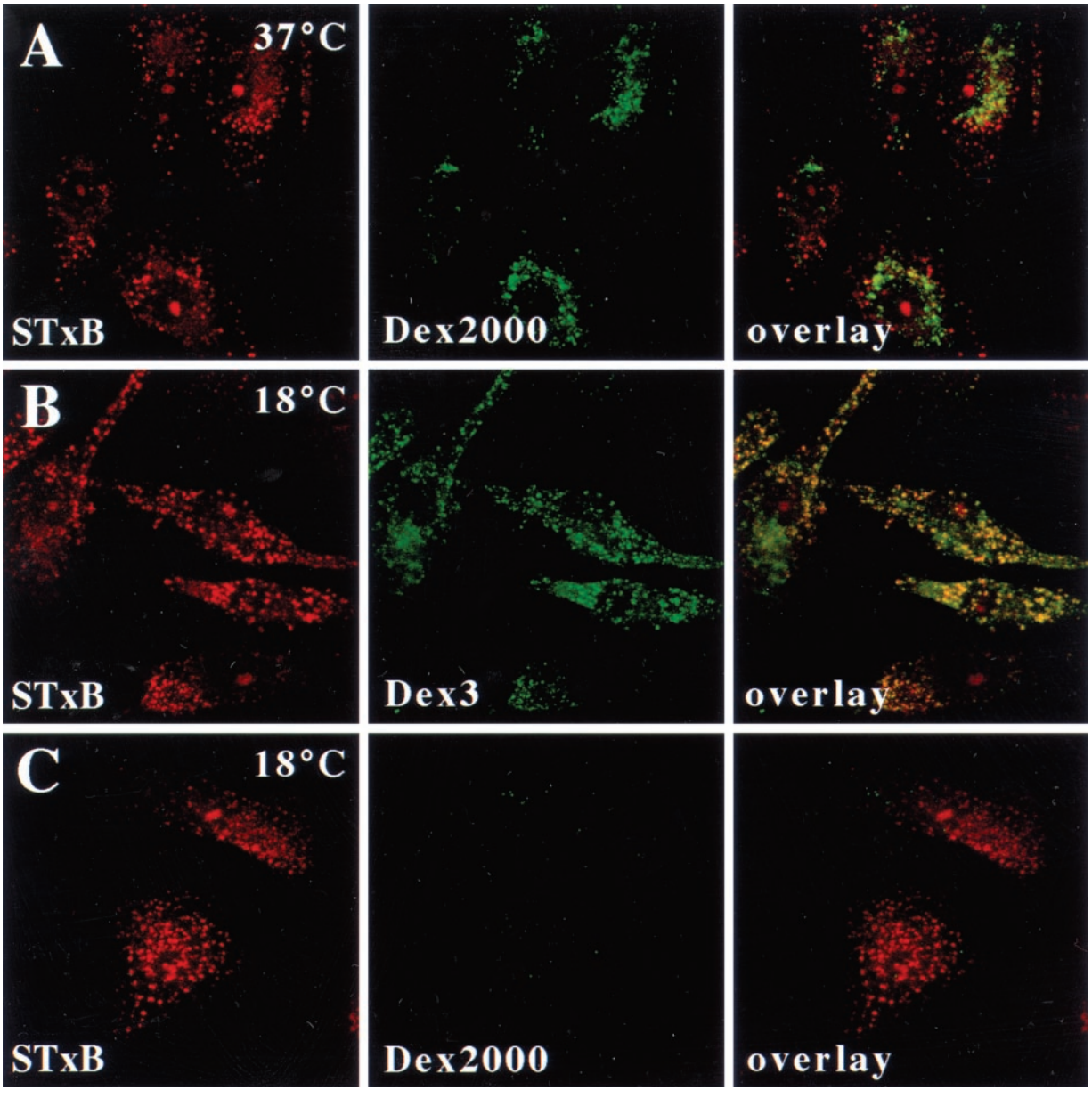

Figure 3. STxB is internalized into macrophages by micropinocytosis. (A–C) STxB (0.1 μM; 5 μg/ml) was cointernalized for 30 min into macrophages with Dex2000 at 37°C (A), with Dex3 at 18°C (B), or with Dex2000 at 19.5°C (C). Cells were then fixed and stained for STxB. Note that STxB extensively colocalized with Dex3, but not with Dex2000.

sion levels, other factors contribute to the transport difference between these cells (see DISCUSSION). Morphological experiments showed that after LPS-treatment, STxB could be visualized in perinuclear membranes of macrophages, where it partly overlapped with the TGN marker TGN46 (Figure 5A, macrophages+LPS). However, as opposed to HeLa cells (Johannes *et al.*, 1997; Mallard *et al.*, 1998) or primary human fibroblasts (Figure 5A), where 45 min after internalization, STxB accumulated primarily in the Golgi apparatus, a number of additional compartments were targeted in LPS-treated macrophages. In summary, the morphological and biochemical data presented above strongly suggested that after its receptor dependent internalization into untreated macrophages and DCs, STxB was not targeted to the biosynthetic/secretory pathway, as opposed to HeLa cells.

Analysis of STxB Association with DRMs in HeLa Cells and Macrophages

Certain membrane microdomains are enriched in (glyco)-sphingolipids, cholesterol, and saturated long-chain glycerophospholipids, and these structures have been ascribed func-

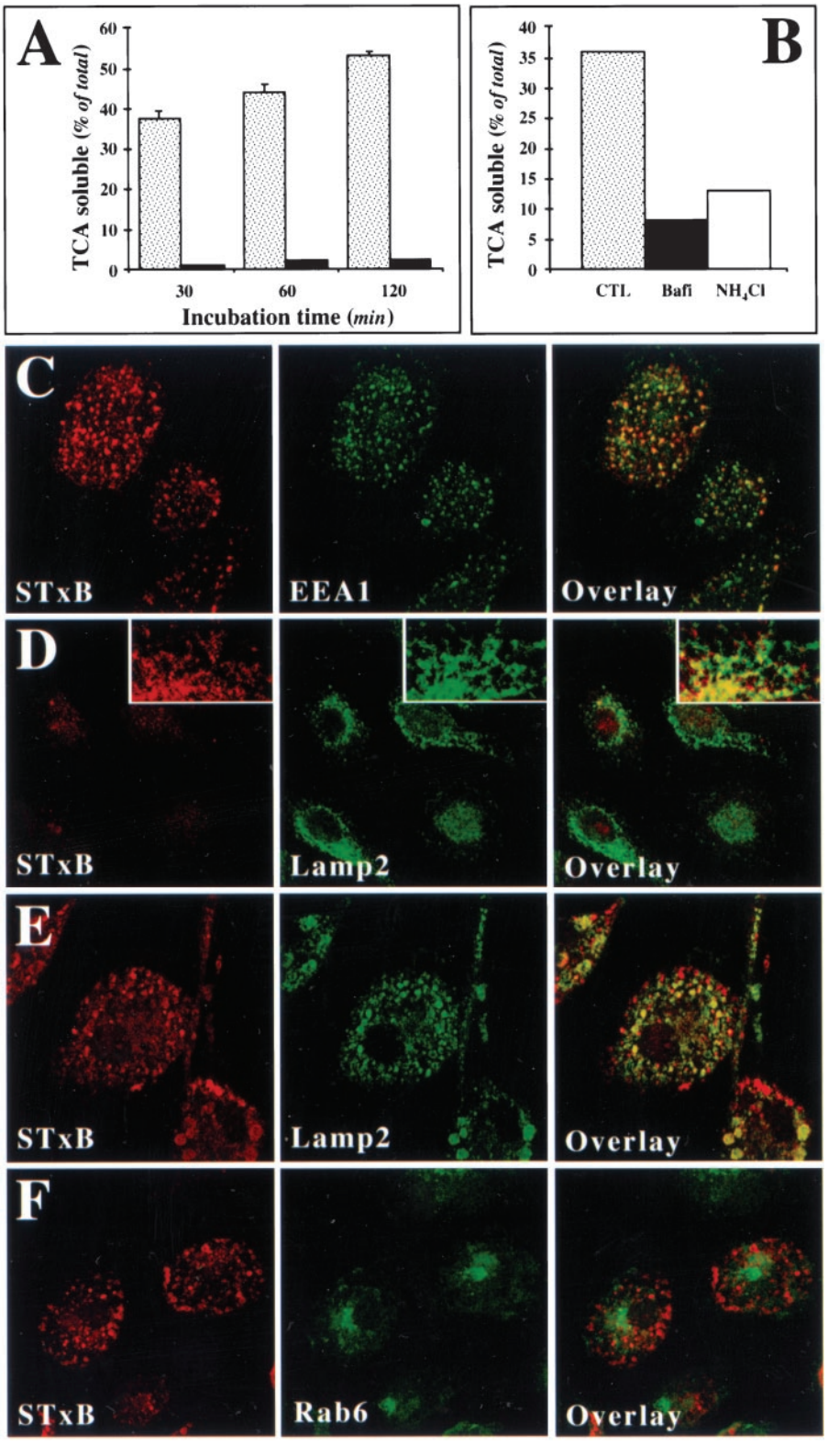

Figure 4. Analysis of STxB transport to the late endocytic pathway in macrophages and DC. (A) Iodinated STxB-Glyc-KDEL (50 nM; 2.5 μg/ml) was incubated for 30 min at 37°C with macrophages (speckled columns) or bound to HeLa cells (■) on ice (A). The cells were then washed on ice, chased at 37°C for the indicated times, and TCA-soluble counts (percentage of the total cell associated radioactivity) were determined. Means (±SEM) of three independent experiments are shown. The appearance of TCA-soluble counts in macrophages indicated that in these cells, STxB was transported to late endosomes/lysosomes. (B) Experiment on macrophages as described in A, in which during the chase period of 30 min, 1 μM Bafi and 50 mM ammonium chloride (NH_4Cl) were added. (C) STxB internalized at 19.5°C colocalized extensively with the early endosomal protein EEA1. STxB was continuously internalized for 1 h. The cells were then fixed and stained with the indicated antibodies. (D) After a 30-min shift to 37°C after internalization at 19.5°C, STxB appeared to be lost from the cells. (Insets) Enhancement of the remaining signal showed a limited codistribution of the remaining STxB labeling with the lysosomal glycoprotein Lamp2, suggesting that STxB might be targeted to lysosomes for degradation. (E) A 30-min shift to 37°C in the presence of Bafi allowed detecting a significant degree of codistribution between STxB and Lamp2. (F) As in E, macrophages were shifted to 37°C in the presence of Bafi and then stained for the indicated proteins. Note that even when STxB degradation was prevented, no significant accumulation in the Golgi region marked by Rab6 could be detected.

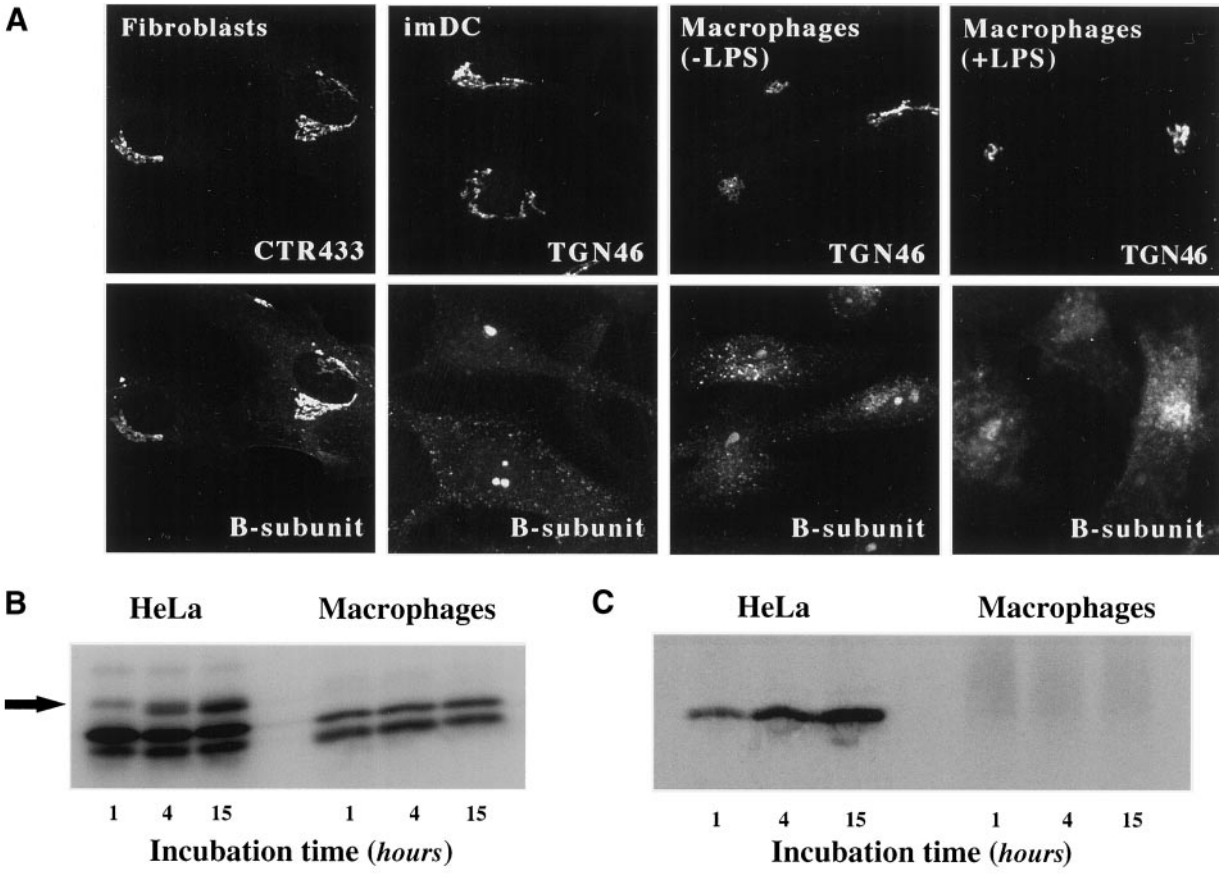

Figure 5. Analysis of STxB transport to the biosynthetic/secretory pathway in macrophages and DC. (A) Immunofluorescence analysis of STxB transport in different primary human cells. Wild-type STxB was internalized constitutively for 45 min at 37°C into macrophages and imDCs, and after binding into fibroblast and LPS-treated macrophages. The cells were then fixed and stained for STxB (bottom) and the Golgi marker CTR433 or the TGN marker TGN46 (top). In macrophages and imDCs, STxB was detected in vesicular cytoplasmic structures, but not in the TGN, whereas in fibroblasts, STxB readily entered the TGN. In LPS-treated macrophages, STxB accumulated in a number of cytoplasmic locations that only partly covered the Golgi region. (B) Glycosylation analysis. Iodinated STxB-Glyc-KDEL (50 nM; 2.5 μg/ml) was internalized after prebinding into HeLa cells or continuously into macrophages for the indicated times. At the end of each incubation period, the cells were lysed and lysates were analyzed by gel electrophoresis. The same numbers of counts were loaded on gels. The arrow indicates the glycosylation product, i.e., ER-localized STxB, which was observed in HeLa cells, but not in macrophages. The lowest bands are proteolytical cleavage products. (C) Sulfation analysis. 0.2 μM of the fusion protein STxB-Sulf$_2$ (10 μg/ml) was internalized after prebinding into HeLa cells or continuously into macrophages for the indicated times in the presence of radioactive sulfate. The cells were then lysed, STxB was immunoprecipitated, and immunoprecipitates were analyzed by gel electrophoresis. Sulfated STxB-Sulf$_2$, i.e., protein that had passed through the TGN, was detected in HeLa cells, but not in macrophages.

tions in membrane sorting (Brown and Rose, 1992; Simons and Ikonen, 1997). Because Gb_3 is a glycosphingolipid, we tested whether STxB bound to its receptor would be associated with DRMs in HeLa cells and macrophages. Radioactive STxB was bound to the plasma membrane of HeLa cells or macrophages, and DRMs were then isolated after lysis in 1% Triton X-100 solution by flotation in an Optiprep step gradient. As shown in Figure 6, the DRM marker GM_1, visualized by cholera toxin binding, was found in both cell types in fraction 2 at the 30/5% interface of the gradient, corresponding to the classical localization of DRMs. Fraction 2 was devoid of TfR immunoreactivity, consistent with the notion that the TfR is not a DRM constituent. In HeLa cells, 27% of cell-associated STxB was recovered from DRM fraction 2, whereas in control and LPS-treated macrophages, STxB in this fraction accounted for only 2 or 5% of cell-associated material, respectively (Figure 6). Protein concentration determination revealed that in macrophages and HeLa cells, fraction 2 contained only 3% of total membrane protein, whereas fractions 5–7 contained >90%. STxB thus appeared to be associated with DRMs in HeLa cells, and not so in macrophages. In agreement with these biochemical data, we also observed in morphological experiments that in HeLa cells, STxB resisted extraction with Triton X-100 (Figure 7; see below), but not in macrophages (our unpublished results).

If STxB association with DRMs was important for retrograde transport in HeLa cells, one would expect the protein to remain associated with DRMs until its arrival in the target compartments of the retrograde route, i.e., the Golgi apparatus and the ER. We therefore analyzed STxB association

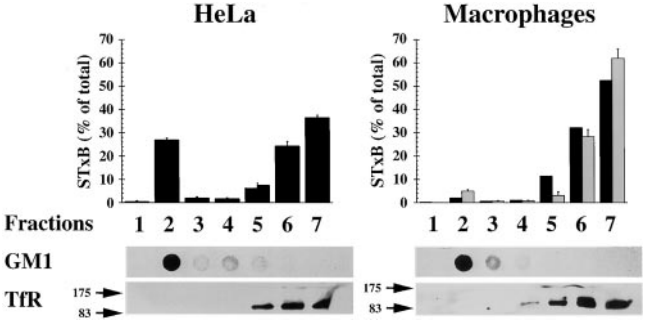

Figure 6. Analysis of STxB association with DRMs. Iodinated STxB (0.2 μM; 10 μg/ml) was bound to control macrophages (■), LPS-treated macrophages (▨), or HeLa cells on ice. The cells were washed, lysed in 1% Triton X-100 buffer, and DRMs were floated in Optiprep step gradients. The gradients were fractionated and the fractions were counted in a gamma counter to determine the distribution of STxB. Furthermore, the fractions were analyzed by dot-blot for GM_1 and by gel electrophoresis for the TfR. Note that in HeLa cells, STxB was readily detected in the DRM fraction 2, whereas association with DRMs was at background levels in non-LPS treated macrophages and only slightly above background in LPS-treated cells. Means of two to four experiments (±SEM) are shown.

with DRMs during retrograde transport (Figure 7). STxB was first internalized at low temperatures into EE (Mallard *et al.*, 1998) (Figure 7A). The cells were then fixed directly (−Triton X-100) or preextracted with Triton X-100 (+Triton X-100) in the cold before fixation and staining for the TfR and GM_1. As mentioned above, the TfR was readily extracted with Triton X-100, whereas GM_1 resisted extraction. EE-associated STxB also resisted the detergent (Figure 7A). Similar results were obtained when Golgi-associated STxB (Figure 7B) or ER-associated STxB-Glyc-KDEL was analyzed (Figure 7C). On detergent extraction, the STxB staining was not lost from the cells. To confirm these experiments, the chimeric STxB mutant STxB-$Sulf_2$, with a tandem sulfation site (Figure 5C), was internalized into HeLa cells in the presence of radioactive sulfate (Figure 7D). The cells were extracted in 1% Triton X-100 solution, and DRMs were obtained by floatation, as described above. Sulfated STxB was found in DRM fraction 2 (Figure 7D), confirming that TGN-located STxB was still in DRMs. Similarly, glycosylated, i.e., ER-associated STxB (Figure 5B) was retrieved from DRM fraction 2 (Figure 7E), suggesting that the protein remained associated with DRMs throughout its retrograde transport to the ER. Interestingly, the colocalization of STxB with BiP in the ER (Figure 8, −TX100) persisted after Triton X-100 extraction (Figure 8, +TX100), again confirming that the detergent-resistant STxB observed under these conditions was ER-associated.

To establish a direct cause-and-effect relationship between DRM association and retrograde transport, we tested whether the destabilization of DRMs by cellular cholesterol extraction would have an effect on STxB transport. Decreasing cellular cholesterol with the use of the cholesterol extraction drug mβCD leads to an inhibition of DRM-dependent endocytosis (Orlandi and Fishman, 1998; Verkade *et al.*, 2000), and our unpublished results show that STxB internalization is abolished under these conditions. However, also the internalization

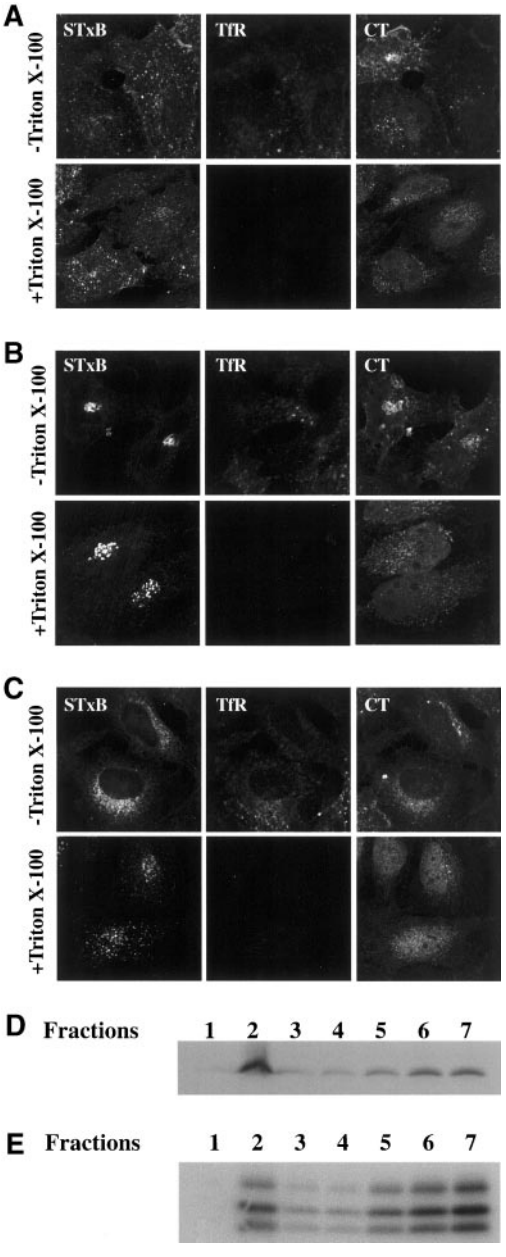

Figure 7. Analysis of STxB association with DRMs along the retrograde pathway. (A–C) Cy3-labeled STxB was internalized for 45 min at 19.5°C (A) or 37°C (B), or Cy3-STxB-Glyc-KDEL (C) for 4 h at 37°C into HeLa cells. The cells were then either fixed directly (−Triton X-100), or preextracted with 1% Triton X-100 solution (+Triton X-100) before fixation. Permeabilized cells were then stained for GM_1 and the TfR. Under these conditions, GM_1 and the EE- (A), Golgi- (B), or ER (C)-associated STxB resisted extraction, whereas the TfR was readily extracted. (D–E) STxB-$Sulf_2$ was internalized in the presence of radioactive sulfate for 45 min at 37°C into HeLa cells (D), and iodinated STxB-Glyc-KDEL was internalized for 15 h (E). The cells were then washed, lysed in 1% Triton X-100 buffer, and DRMs were floated in Optiprep step gradients. The gradients were fractionated, STxB in the fractions was immunoprecipitated with 13C4 antibody, and immunoprecipitates were analyzed by gel electrophoresis. DRM fraction 2 contained a significant amount of the sulfated (D) or glycosylated (E; uppermost bands) STxB.

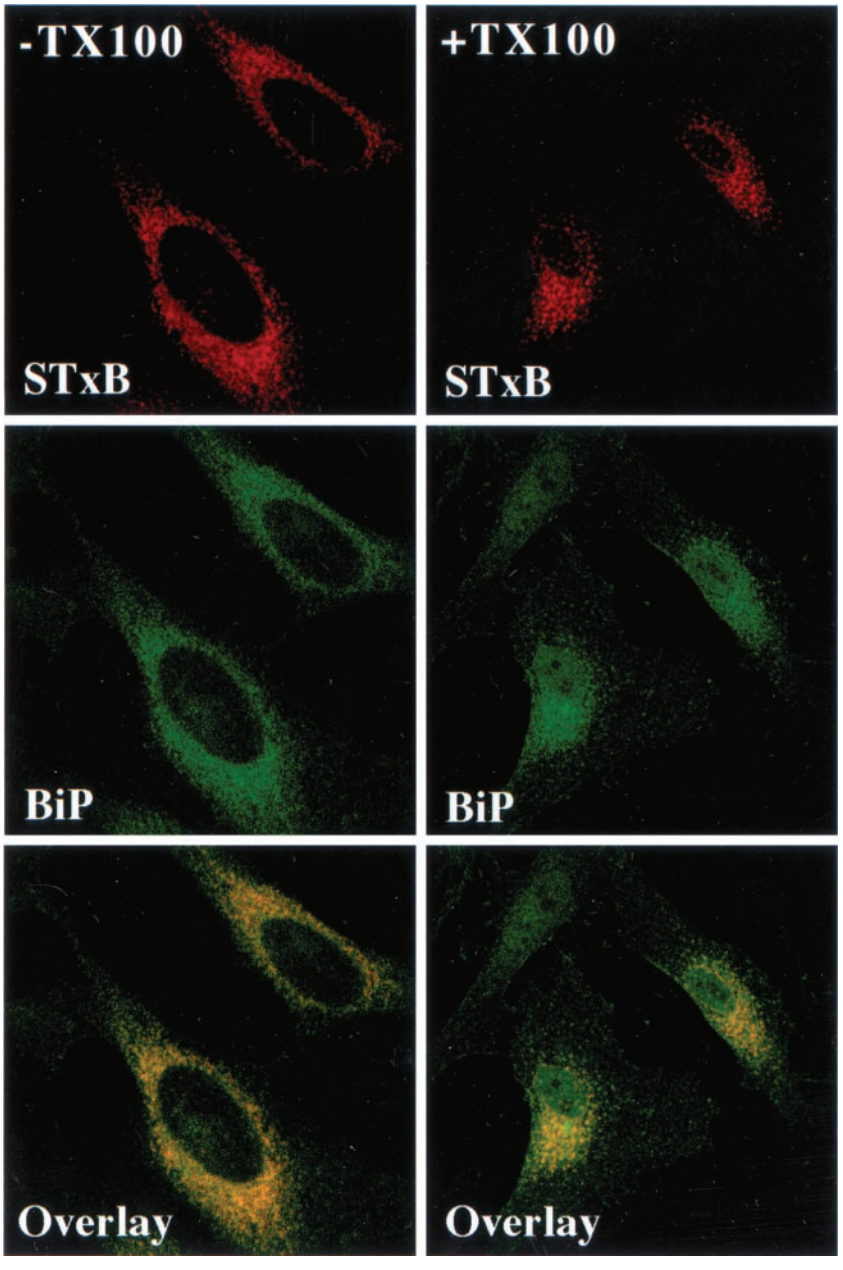

Figure 8. STxB and BiP colocalize even after extraction with Triton X-100. Cy3-coupled STxB-Glyc-KDEL was bound to the plasma membrane of HeLa cells on ice. The cells were washed, shifted to 37°C for 4 h, placed on ice, incubated (+TX100) or not (−TX100) for 1 min in 1% Triton X-100-containing buffer, and then fixed at room temperature for 15 min. The fixed and permeabilized (saponin) cells were incubated with the indicated antibodies, mounted in Mowiol, and viewed by confocal microscopy. Note that even after extraction with Triton X-100, BiP labeling colocalized with STxB-Glyc-KDEL-specific labeling.

of the TfR, a non-DRM constituent, is inhibited by cholesterol extraction (Rodal *et al.*, 1999; Subtil *et al.*, 1999), indicating that at the plasma membrane, DRM destabilization is not sufficient to explain the effects of the drug. To measure specifically EE-to-TGN transport, STxB-Sulf$_2$ (Figure 5C) was internalized at 19.5°C into EE of HeLa cells (Mallard *et al.*, 1998). The cells were then treated for 1 h with mβCD to reduce cellular free cholesterol levels to 72% of mock-treated cells (Figure 9B). With the use of STxB coupled to biotin via a reducible disulfide bond (see MATERIALS AND METHODS), it was verified that under both conditions, similar amounts of STxB were inside the cells (Figure 9, A and B). The cells were then shifted for 30 min to 37°C in the presence of radioactive sulfate, and after subsequent immunoprecipitation, sulfated STxB was analyzed by gel electrophoresis and autoradiography. It was found that in cholesterol extracted cells, STxB transport to the TGN was reduced to 62% of control levels (Figure 9B). It thus appeared that STxB transport to the TGN was sensible to the cellular cholesterol homeostasis.

To investigate the role of DRMs in EE-to-TGN transport even more directly, a newly established experimental system was used which reconstitutes this step on SLO-permeabilized HeLa cells (Mallard, Tang, Galli, Yue, Tenza, Antony, Goud, Hong, and Johannes, unpublished data) (Figure 10). STxB-Sulf$_2$ was internalized at low temperatures into EE of intact cells (Mallard *et al.*, 1998) (Figure 10C,

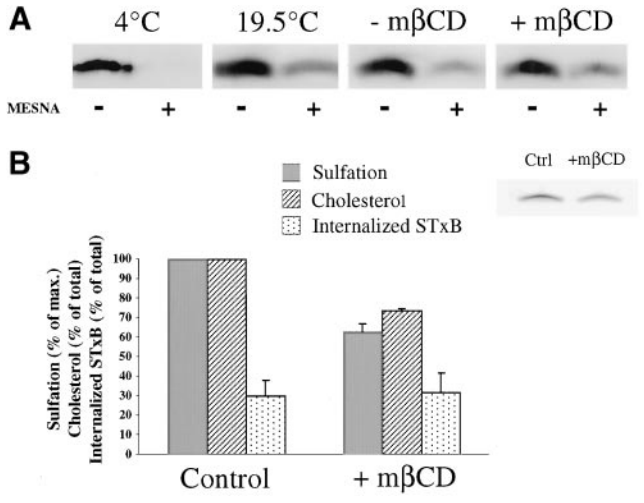

Figure 9. EE-to-TGN transport is inhibited under cholesterol extraction conditions. (A) Biotinylated STxB mutant was bound to HeLa cells on ice (condition 4°C) or internalized at 19.5°C into EE (conditions 19.5°C, −mβCD, +mβCD). The cells were then either directly placed on ice (4 and 19.5°C), or incubated with (+mβCD) or without (−mβCD) 10 mM mβCD for 60 min at 19.5°C before passage on ice. After MESNA (+) or mock (−) treatment on ice, the cells were lysed and biotinylated STxB was detected by Western. (B) STxB-Sulf$_2$ was internalized and cholesterol was extracted as described in A. Cells were then used to determine the amount of free cellular cholesterol (control cells contained 7.93 ± 1.88 μg of cholesterol/10^6 cellules) or were shifted to 37°C for 30 min in the presence of radioactive sulfate. Note that transport to the TGN (sulfation) was significantly inhibited by cholesterol extraction. The inset shows a typical result of the sulfation reactions in the −mβCD and the +mβCD conditions.

protocol 1). The plasma membrane of these cells was then selectively permeabilized with SLO, endogenous cytosol was allowed to leak out for 10 min, and cellular cholesterol was extracted from permeabilized cells for 15 min with the use of the increasing doses of mβCD (Figure 10A). Importantly, DRMs were destabilized under these conditions because STxB (Figure 10B) and GM_1 (our unpublished results) association with the DRM-fraction 2 was reduced in a dose-dependent manner. The SLO-permeabilized and mock-extracted or cholesterol-extracted cells were then incubated for 30 min at 37°C in the presence of exogenous HeLa cytosol, ATP-regenerating system, and radioactive sulfate for detection of STxB arrival in the TGN (Figure 10C, protocol 1). Sulfated STxB was then immunoprecipitated and analyzed by gel electrophoresis and autoradiography. The sulfation signal obtained in the presence of cytosol and the absence of cholesterol extraction was set to 100% (Figure 10D).

A tight correlation was observed between DRM destabilization (Figure 10B) through cholesterol extraction (Figure 10A) and inhibition of transport to the TGN (Figure 10D). In fact, when DRMs were completely destabilized (10 mM mβCD), STxB transport to the TGN was reduced to background levels, as defined by transport in the absence of exogenous cytosol. mβCD (2.5 and 5 mM) had intermediate effects. Importantly, sulfation of TGN-localized STxB (Figure 10C, protocol 2; for results, see inset) and of endogenous proteins and proteoglycans (see MATERIALS AND METHODS) was only very little affected by cholesterol extraction, indicating that mβCD did not simply render the cells or the sulfotransferase inactive. The functionality of the cholesterol-extracted cells was further confirmed by the following experiment. Radiolabeled Tf instead of STxB-Sulf$_2$ was internalized into HeLa cells at 19.5°C. The cells were then permeabilized as described above, and after the 30-min incubation period at 37°C, Tf that was released from the permeabilized cells was quantified (Figure 10E). This release process was cytosol (Advani *et al.*, 1999) and energy-dependent. Importantly, even at high doses (10 mM), mβCD extraction did not inhibit Tf recycling (Figure 10E) as previously observed in intact cells (Subtil *et al.*, 1999). In conclusion, these experiments strongly suggest that the integrity of DRMs is a prerequisite for STxB targeting into the retrograde transport route.

The specificity of the cholesterol extraction reaction was confirmed by the demonstration that cholesterol back-addition to extracted cells allowed to restore transport (Figure 10, F and G). After SLO binding on ice, HeLa cells were immediately incubated for 10 min at 37°C in the presence of 10 mM of mβCD, and it was verified that even under these conditions, permeabilization still occurred. The cells were then further incubated for 10 min at 37°C in the presence of the indicated concentrations of cholesterol-saturated mβCD, conditions that allowed a dose-dependent back-addition of cholesterol (Figure 10G). At higher concentrations, i.e., >1 mM, the cellular membranes were even overloaded with cholesterol. STxB reassociation with DRMs under these conditions is currently under study. The transport reaction revealed that cholesterol back-addition first reversed the inhibitory effect of depletion (Figure 10F). At high doses, however, transport was inhibited again, suggesting that optimal transport to the TGN required a precise regulation of early endosomal cholesterol levels.

DISCUSSION

We have compared STxB intracellular transport in monocyte-derived cells to that previously described in HeLa cells. In untreated monocyte-derived cells, targeting to the biosynthetic/secretory pathway did not occur, as opposed to HeLa cells. This difference could be correlated with our finding that in HeLa cells, STxB associated with DRMs, but not in monocyte-derived cells, suggesting that DRM association is a prerequisite for targeting into the retrograde route. Accordingly, we observed that in HeLa cells, STxB remained associated with DRMs until its arrival in the target compartments of the retrograde transport route, i.e., the Golgi apparatus and the endoplasmic reticulum, and the destabilization of DRMs by cholesterol extraction strongly inhibited retrograde transport of STxB.

A clue to understanding the differences in STxB trafficking in monocyte-derived cells, compared with HeLa cells, came from our observation that STxB appeared to be associated with DRMs in HeLa cells, but not in monocytes and macrophages. Several possibilities exist to explain this difference. First, the expression of Gb_3 in monocyte-derived cells was found to be lower than in HeLa cells. If STxB-dependent Gb_3 clustering was important for targeting to the DRMs then lower Gb_3 expression at the plasma membrane might lead to inefficient clustering. Our data indicate that Gb_3 expression

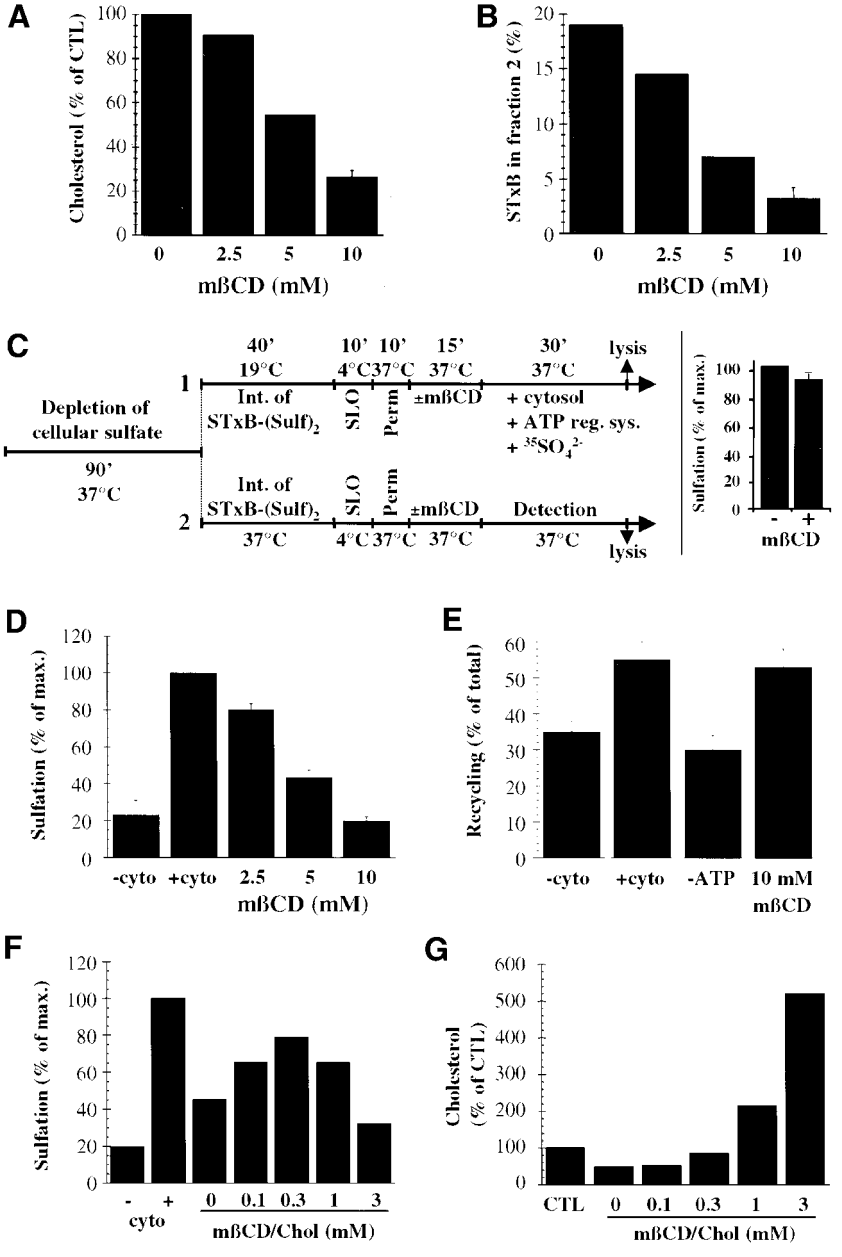

Figure 10. Establishment of a cause-and-effect relationship between STxB association with DRMs and its transport from EE to the TGN. (A) A 15-min treatment at 37°C of SLO-permeabilized HeLa cells with the indicated doses of mβCD led to a dose-dependent extraction of free cellular cholesterol. The means of two to three experiments are shown. Nontreated SLO-permeabilized cells had 5 μg of cholesterol/10^6 cells. (B) Cholesterol extraction displaces STxB from DRM fraction 2. Note that STxB association with fraction 2 is lower than in Figure 6 due to an additional incubation at 37°C for cholesterol extraction (see MATERIALS AND METHODS). The means of two to three experiments are shown. (C) Generic protocols used to reconstitute EE-to-TGN transport of STxB. Perm., permeabilization in intracellular transport buffer/dithiothreitol at 37°C (see MATERIALS AND METHODS). Detection: incubation of permeabilized cells with radioactive sulfate in the absence of cytosol. Protocol 1: standard protocol (see below, D). Protocol 2: Comparison of sulfation efficiencies on TGN-localized STxB (40 min transport at 37°C in intact cells) in SLO-permeabilized and mβCD- or mock-treated cells (for results, see insert; means of three experiments). (D) STxB transport from EE to the TGN on SLO-permeabilized cells is inhibited when DRMs are destabilized by 15-min extraction of cellular cholesterol with the indicated doses of mβCD. Transport efficiency in the presence of cytosol is put to 100%. The means (± SEM) of three to six experiments are shown. (E) ATP- and cytosol-dependent Tf recycling to the plasma membrane is not affected by cellular cholesterol extraction. The percentage of released Tf over total cell associated Tf was determined, and the means (± SEM) of 6–10 experiments are shown. **(F)** Cholesterol back-addition. In a variation of protocol 1 (C), the cells were extracted for 10 min at 37°C with 10 mM mβCD from permeabilization on, incubated for 10 min at 37°C with the indicated concentrations of cholesterol-saturated mβCD, and then shifted for 30 min to 37°C in the presence of cytosol and radioactive sulfate. Note that cholesterol back addition partially rescued transport to the TGN. (G) Quantification of cholesterol back-addition. The quantities of total free cellular cholesterol under the indicated conditions were determined. In F and G, a representative of two experiments is shown.

might in fact, in part, be a factor that determines targeting to the retrograde route, because increased Gb_3 expression in LPS-treated macrophages and monocytes also allowed to detect STxB targeting to the Golgi apparatus and the ER. We have found, however, that even when Gb_3 expression was equivalent, retrograde transport in monocytes and macrophages was still five- to sevenfold less efficient than in HeLa cells. This observation suggests that Gb_3 density is not sufficient to explain the difference between both cell types. Second, it has been suggested that certain Gb_3 isoforms are preferentially associated with retrograde transport (Sandvig *et al.*, 1994; Sandvig *et al.*, 1996; Arab and Lingwood, 1998). Thus, HeLa cells may express those Gb_3 isoforms that allow DRM association, whereas macrophages or DCs do not. Van Setten *et al.* (1996) in fact provided evidence for the expression of an alternative Gb_3 isoform in primary human monocytes, and further work is required to reveal the molecular identity of this lipid. The isoform hypothesis is tempting in light of recent data from Maxfield and colleagues who documented isoform-specific differences in the sorting of lipid analogs in the endocytic membrane system (Mukherjee *et al.*, 1999). Third, membrane composition and dynamics of macrophages and DCs might be distinct from that of HeLa cells. It has, for example, recently been shown that differences in cholesterol content of cellular membranes can have major effects on trafficking through endosomes (Kobayashi *et al.*, 1999; Puri *et al.*, 1999; Grimmer *et al.*, 2000). It should be noted, however, that GM_1 was also found in DRMs of mac-

rophages and DCs, showing that at least some aspects of DRM dynamics are comparable between HeLa cells and macrophages. Whether differential association with DRMs is the sole explanation for the transport differences between human monocyte-derived cells and HeLa cells remains to be determined.

A central function of DRMs in membrane sorting in the biosynthetic/secretory pathway has previously been suggested (reviewed by Simons and Ikonen, 1997), and more recently direct evidence shown for the existence of DRMs in the plasma membrane (Friedrichson and Kurzchalia, 1998; Harder *et al.*, 1998; Varma and Mayor, 1998). Furthermore, lateral lipid asymmetry in endosomes has been deduced from the observation that glycosyl phosphatidyl inositol-anchored proteins recycle more readily after cholesterol extraction (Mayor *et al.*, 1998), and that the recycling compartment is rich in DRM components (Gagescu *et al.*, 2000). With the use of a newly developed assay system, we have found here that transfer from EE to the TGN was perturbed when DRMs were destabilized by cellular cholesterol extraction. Furthermore, STxB was associated with DRMs not only in the early endosomal donor compartment but also in the target compartment, i.e., the TGN. These data extend the DRM hypothesis on membrane trafficking and suggest that lipid repartition-dependent sorting might play a central role in the retrograde transport pathway.

The targeting of STxB to the ER in association with DRMs may appear surprising because it is traditionally thought that the ER, due to its low levels in cholesterol, does not favor the formation of DRMs (reviewed in Muniz and Riezman, 2000). However, it has recently been shown that some yeast proteins become detergent-insoluble in the ER (Bagnat *et al.*, 2000), indicating the possibility of the existence of DRMs in this compartment. The retrograde targeting of DRMs to the ER might provide a structural basis for the COPI-independent Golgi-to-ER transport route that has recently been uncovered with the use of, among others, STxB as a tool (Girod *et al.*, 1999; White *et al.*, 1999).

It appears of interest that the TfR, which colocalizes with STxB in EE (Mallard *et al.*, 1998), but which is not transported to the Golgi apparatus, is also not found in DRMs. As opposed to its internalization (Rodal *et al.*, 1999; Subtil *et al.*, 1999; our unpublished observations), TfR recycling was found not to be inhibited by cholesterol extraction with mβCD on permeabilized cells (our study) or intact cells (Subtil *et al.*, 1999). This might point to fundamental differences between both TfR transport steps, such as clathrin/AP2 function in internalization (Benmerah *et al.*, 1998), but not in recycling (Marsh *et al.*, 1995). At the level of EE, we have previously shown that the TfR and STxB were accumulated in overlapping, but often distinct membrane profiles (Mallard *et al.*, 1998), and it may be speculated that such segregation resulted from localization of both proteins to distinct membrane microdomains.

Even although the key sorting step in the retrograde transport route is at the level of EE, STxB associated with DRMs already at the plasma membrane. In agreement with this finding, we also observed that cholesterol extraction strongly inhibited STxB internalization. It might then be suggested that STxB targeting to the retrograde route is already preprogrammed at the plasma membrane through the protein's association with DRMs. In agreement with this hypothesis we found, with the use of a dominant negative mutant of Eps15, that STxB transport to the TGN/Golgi apparatus is independent of adaptor protein-2/clathrin function (Wiltz and Johannes, unpublished data), suggesting that in addition to clathrin-dependent endocytosis (Sandvig *et al.*, 1989), STxB can enter cells by clathrin-independent endocytosis, which appears to determine targeting to the retrograde transport route. It appears in fact likely that not only STxB but also other toxins (Orlandi and Fishman, 1998) and receptors, such as the interferon receptors (Zoon *et al.*, 1983; Takaoka *et al.*, 2000) can take several entry pathways that, in fine, may determine their transport to alternate intracellular destinations.

In conclusion, this study reveals the importance of lipid asymmetry in the retrograde transport pathway and identifies STxB as a convenient model for the study of this phenomenon. Further work is required to identify the molecular details of the lipid environment required for membrane sorting at the EE/TGN interface.

ACKNOWLEDGMENTS

We thank Philippe Benaroch (Institut Curie, Paris, France) for critical reading of the manuscript and Christophe Lamaze (Institut Pasteur, Paris, France) for helpful discussion; Beth Boyd (Hospital for Sick Children, Toronto, Canada), Claude Wolf, and Odile Colard (Center Hospitalier Universitaire St. Antoine, Paris, France) for help with the lipid extraction experiments; Emmanuelle Bismuth and Lucien Cabanié (Institut Curie, Paris, France) for expert protein purification; and Jürgen Benting (EMBL, Heidelberg, Germany) for protocols on DRM purification. We are indebted to Françoise Raynaud (Faculté des Sciences Pharmaceutiques et Biologiques, Paris, France) for primary fibroblasts, to Rainer Pepperkok (EMBL, Heidelberg, Germany) for the anti-TGN46 antibody, and to the Genetics Institute (Cambridge, MA) for recombinant human colony stimulating factor-1. This work was supported by grants to L.J. from the Association pour la Recherche sur le Cancer (no. 9028) and the Ligue Nationale contre le Cancer.

REFERENCES

Abe, A., Inokuchi, J., Jimbo, M., Shimeno, H., Nagamatsu, A., Shayman, J.A., Shukla, G.S., and Radin, N.S. (1992). Improved inhibitors of glucosylceramide synthase. J. Biochem. *111*, 191–196.

Advani, R.J., Yang, B., Prekeris, R., Lee, K.C., Klumperman, J., and Scheller, R.H. (1999). VAMP-7 mediates vesicular transport from endosomes to lysosomes. J. Cell Biol. *146*, 765–776.

Arab, S. and Lingwood, C.A. (1998) Intracellular targeting of the endoplasmic reticulum/nuclear envelope by retrograde transport may determine cell hypersensitivity to verotoxin via globotriaosyl ceramide fatty acid isoform traffic. J. Cell Physiol. *177*, 646–660.

Bagnat, M., Keranen, S., Shevchenko, A., and Simons, K. (2000). Lipid rafts function in biosynthetic delivery of proteins to the cell surface in yeast. Proc. Natl. Acad. Sci. USA *97*, 3254–3259.

Banchereau, J., and Steinman, R.M. (1998) Dendritic cells and the control of immunity. Nature *392*, 245–252.

Baron, C.L., Raposo, G., Scholl, S.M., Bausinger, H., Tenza, D., Bohbot, A., Pouillart, P., Goud, B., Hanau, D., and Salamero, J. (2001). Modulation of MHC class II transport and lysosome distribution by macrophage-colony stimulating factor in human dendritic cells derived from monocytes. J. Cell Sci. *114*, 999–1010.

Benmerah, A., Lamaze, C., Begue, B., Schmid, S.L., Dautry-Varsat, A., and Cerf-Bensussan, N. (1998). AP-2/Eps15 interaction is re-

quired for receptor-mediated endocytosis. J. Cell Biol. *140*, 1055–1062.

Benting, J.H., Rietveld, A.G., and Simons, K. (1999). N-Glycans mediate the apical sorting of a GPI-anchored, raft-associated protein in Madin-Darby canine kidney cells. J. Cell Biol. *146*, 313–320.

Bligh, E.G. and Dyer, W.J. (1959) A rapid method of total lipid extraction and purification. Can. J. Biochem. Biophys. *37*, 911–917.

Brown, D.A. and London, E. (1998) Functions of lipid rafts in biological membranes. Annu. Rev. Cell Dev. Biol. *14*, 111–136.

Brown, D.A. and Rose, J.K. (1992) Sorting of GPI-anchored proteins to glycolipid-enriched membrane subdomains during transport to the apical cell surface. Cell *68*, 533–544.

Clague, M.J., Urbe, S., Aniento, F., and Gruenberg, J. (1994). Vacuolar ATPase activity is required for endosomal carrier vesicle formation. J. Biol. Chem. *269*, 21–24.

Dimon-Gadal, S., Raynaud, F., Evain-Brion, D., and Keryer, G. (1998). MAP kinase abnormalities in hyperproliferative cultured fibroblasts from psoriatic skin. J. Invest. Dermatol. *110*, 872–879.

Faradji, A., Bohbot, A., Schmitt-Goguel, M., Siffert, J.C., Dumont, S., Wiesel, M.L., Piemont, Y., Eischen, A., Bergerat, J.P., Bartholeyns, J., Poindron, P., Witz, J.P., and Oberling, F. (1994) Large scale isolation of human blood monocytes by continuous flow centrifugation leukapheresis and counterflow centrifugation elutriation for adoptive cellular immunotherapy in cancer patients. J. Immunol. Methods *174*, 297–309.

Friedrichson, T., and Kurzchalia, T.V. (1998) Microdomains of GPI-anchored proteins in living cells revealed by crosslinking. Nature *394*, 802–805.

Gagescu, R., Demaurex, N., Parton, R.G., Hunziker, W., Huber, L.A., and Gruenberg, J. (2000). The recycling endosome of Madin-Darby canine kidney cells is a mildly acidic compartment rich in raft components. Mol. Biol. Cell *11*, 2775–2791.

Galli, T., Chilcote, T., Mundigl, O., Binz, T., Niemann, H., and De Camilli, P. (1994). Tetanus toxin-mediated cleavage of cellubrevin impairs exocytosis of transferrin receptor-containing vesicles in CHO cells. J. Cell Biol. *125*, 1015–1024.

Gamble, W., Vaughan, M., Kruth, H.S., and Avigan, J. (1978). Procedure for determination of free and total cholesterol in micro- or nanogram amounts suitable for studies with cultured cells. J. Lipid Res. *19*, 1068–1070.

Garrett, W.S., Chen, L.M., Kroschewski, R., Ebersold, M., Turley, S., Trombetta, S., Galan, J.E., and Mellman, I. (2000). Developmental control of endocytosis in dendritic cells by Cdc42. Cell *102*, 325–334.

Ghosh, R.N., Mallet, W.G., Soe, T.T., McGraw, T.E., and Maxfield, F.R. (1998). An endocytosed TGN38 chimeric protein is delivered to the TGN after trafficking through the endocytic recycling compartment in CHO cells. J. Cell Biol. *142*, 923–936.

Girod, A., Storrie, B., Simpson, J.C., Johannes, L., Goud, B., Roberts, L.M., Lord, J.M., Nilsson, T., and Pepperkok, R. (1999). Evidence for a COP-I-independent transport route from the Golgi complex to the endoplasmic reticulum. Nat. Cell Biol. *1*, 423–430.

Grimmer, S., Iversen, T.G., van Deurs, B., and Sandvig, K. (2000). Endosome to golgi transport of ricin is regulated by cholesterol. Mol. Biol. Cell *11*, 4205–4216.

Haicheur, N., Bismuth, E., Bosset, S., Adotevi, O., Warnier, G., Lacabanne, V., Regnault, A., Desaymard, C., Amigorena, S., Riccardi-Castagnoli, P., Goud, B., Fridman, W.-H., Johannes, L., and Tartour, E. (2000) The B-subunit of Shiga toxin fused to a tumor antigen elicits CTL and targets dendritic cells to allow MHC class I restricted presentation of peptides derived from exogenous antigens. J. Immunol. *165*, 3301–3308.

Hakomori, S., Yamamura, S., and Handa, A.K. (1998). Signal transduction through glyco(sphingo)lipids. Introduction and recent studies on glyco(sphingo)lipid-enriched microdomains. Ann. NY Acad. Sci. *845*, 1–10.

Harder, T., Scheiffele, P., Verkade, P., and Simons, K. (1998). Lipid domain structure of the plasma membrane revealed by patching of membrane components. J. Cell Biol. *141*, 929–942.

Hart, D.N. (1997). Dendritic cells: unique leukocyte populations which control the primary immune response. Blood *90*, 3245–3287.

Hazes, B., and Read, R.J. (1997) Accumulating evidence suggests that several AB-toxins subvert the endoplasmic reticulum-associated protein degradation pathway to enter target cells. Biochemistry *36*, 11051–11054.

Hooper, N.M. (1999). Detergent-insoluble glycosphingolipid/cholesterol-rich membrane domains, lipid rafts and caveolae. Mol. Membr. Biol. *16*, 145–156.

Johannes, L. and Goud, B. (1998) Surfing on a retrograde wave: how does Shiga toxin reach the endoplasmic reticulum? Trends Cell Biol. *8*, 158–162.

Johannes, L., Tenza, D., Antony, C., and Goud, B. (1997). Retrograde transport of KDEL-bearing B-fragment of Shiga toxin. J. Biol. Chem. *272*, 19554–19561.

Khine, A.A., and Lingwood, C.A. (1994) Capping and receptor-mediated endocytosis of cell-bound verotoxin (Shiga-like toxin). 1: Chemical identification of an amino acid in the B subunit necessary for efficient receptor glycolipid binding and cellular internalization. J. Cell Physiol. *161*, 319–332.

Kobayashi, T., Beuchat, M.H., Lindsay, M., Frias, S., Palmiter, R.D., Sakuraba, H., Parton, R.G., and Gruenberg, J. (1999). Late endosomal membranes rich in lysobisphosphatidic acid regulate cholesterol transport. Nat. Cell Biol. *1*, 113–118.

Lee, R.-S., Tartour, E., van der Bruggen, P., Vantomme, V., Goud, B., Fridman, W.-H., and Johannes, L. (1998). Major histocompatibility complex class I presentation of exogenous soluble tumor antigen fused to the B-fragment of Shiga toxin. Eur. J. Immunol. *28*, 2726–2737.

Lingwood, C.A. (1993). Verotoxins and their glycolipid receptors. Adv. Lipid Res. *25*, 189–211.

Lingwood, C.A., Law, H., Richardson, S., Petric, M., Brunton, J.L., De Grandis, S., and Karmali, M. (1987). Glycolipid binding of purified and recombinant *Escherichia coli* produced verotoxin in vitro. J. Biol. Chem. *262*, 8834–8839.

Mallard, F., Tenza, D., Antony, C., Salamero, J., Goud, B., and Johannes, L. (1998). Direct pathway from early/recycling endosomes to the Golgi apparatus revealed through the study of Shiga toxin B-fragment transport. J. Cell Biol. *143*, 973–990.

Marsh, E.W., Leopold, P.L., Jones, N.L., and Maxfield, F.R. (1995). Oligomerized transferrin receptors are selectively retained by a lumenal sorting signal in a long-lived endocytic recycling compartment. J. Cell Biol. *129*, 1509–1522.

Mayor, S., Sabharanjak, S., and Maxfield, F.R. (1998). Cholesterol-dependent retention of GPI-anchored proteins in endosomes. EMBO J. *17*, 4626–4638.

Mellman, I., Turley, S.J., and Steinman, R.M. (1998). Antigen processing for amateurs and professionals. Trends Cell Biol. *8*, 231–237.

Mukherjee, S., Soe, T.T., and Maxfield, F.R. (1999). Endocytic sorting of lipid analogues differing solely in the chemistry of their hydrophobic tails. J. Cell Biol. *144*, 1271–1284.

Muniz, M., and Riezman, H. (2000) Intracellular transport of GPI-anchored proteins. EMBO J. *19*, 10–15.

O'Brien, A.D., Tesh, V.L., Donohue-Rolfe, A., Jackson, M.P., Olsnes, S., Sandvig, K., Lindberg, A.A., and Keusch, G.T. (1992). Shiga toxin: biochemistry, genetics, mode of action, and role in pathogenesis. Curr. Top. Microbiol. Immunol. *180*, 65–94.

Orlandi, P.A. and Fishman, P.H. (1998) Filipin-dependent inhibition of cholera toxin: evidence for toxin internalization and activation through caveolae-like domains. J. Cell Biol. *141*, 905–915.

Peters, J.H., Gieseler, R., Thiele, B., and Steinbach, F. (1996). Dendritic cells: from ontogenetic orphans to myelomonocytic descendants. Immunol. Today *17*, 273–278.

Pratten, M.K., and Lloyd, J.B. (1979) Effects of temperature, metabolic inhibitors and some other factors on fluid-phase and adsorptive pinocytosis by rat peritoneal macrophages. Biochem. J. *180*, 567–571.

Puri, V., Watanabe, R., Dominguez, M., Sun, X., Wheatley, C.L., Marks, D.L., and Pagano, R.E. (1999). Cholesterol modulates membrane traffic along the endocytic pathway in sphingolipid-storage diseases. Nat. Cell Biol. *1*, 386–388.

Ramegowda, B., and Tesh, V.L. (1996) Differentiation-associated toxin receptor modulation, cytokine production, and sensitivity to Shiga-like toxins in human monocytes and monocytic cell lines. Infect. Immun. *64*, 1173–1180.

Rodal, S.K., Skretting, G., Garred, O., Vilhardt, F., van Deurs, B., and Sandvig, K. (1999). Extraction of cholesterol with methyl-beta-cyclodextrin perturbs formation of clathrin-coated endocytic vesicles. Mol. Biol. Cell *10*, 961–974.

Sallusto, F., Cella, M., Danieli, C., and Lanzavecchia, A. (1995). Dendritic cells use macropinocytosis and the mannose receptor to concentrate macromolecules in the major histocompatibility complex class II compartment: downregulation by cytokines and bacterial products. J. Exp. Med. *182*, 389–400.

Sallusto, F., and Lanzavecchia, A. (1994) Efficient presentation of soluble antigen by cultured human dendritic cells is maintained by granulocyte/macrophage colony-stimulating factor plus interleukin 4 and downregulated by tumor necrosis factor alpha. J. Exp. Med. *179*, 1109–1118.

Sandvig, K., Garred, O., Prydz, K., Kozlov, J.V., Hansen, S.H., and van Deurs, B. (1992). Retrograde transport of endocytosed Shiga toxin to the endoplasmic reticulum. Nature *358*, 510–512.

Sandvig, K., Garred, O., van Helvoort, A., van Meer, G., and van Deurs, B. (1996). Importance of glycolipid synthesis for butyric acid-induced sensitization to shiga toxin and intracellular sorting of toxin in A431 cells. Mol. Biol. Cell *7*, 1391–1404.

Sandvig, K., Olsnes, S., Brown, J.E., Petersen, O.W., and van Deurs, B. (1989). Endocytosis from coated pits of Shiga toxin: a glycolipid-binding protein from *Shigella dysenteriae* 1. J. Cell Biol. *108*, 1331–1343.

Sandvig, K., Ryd, M., Garred, O., Schweda, E., Holm, P.K., and van Deurs, B. (1994). Retrograde transport from the Golgi complex to the ER of both Shiga toxin and the nontoxic Shiga B-fragment is regulated by butyric acid and cAMP. J. Cell Biol. *126*, 53–64.

Sandvig, K. and van Deurs, B. (1996) Endocytosis, intracellular transport, and cytotoxic action of Shiga toxin and ricin. Physiol. Rev. *76*, 949–966.

Simons, K. and Ikonen, E. (1997) Functional rafts in cell membranes. Nature *387*, 569–572.

Simpson, J.C., Roberts, L.M., Romisch, K., Davey, J., Wolf, D.H., and Lord, J.M. (1999). Ricin A chain utilizes the endoplasmic reticulum-associated protein degradation pathway to enter the cytosol of yeast. FEBS Lett. *459*, 80–84.

Strockbine, N.A., Marques, L.R., Holmes, R.K., and O'Brien, A.D. (1985). Characterization of monoclonal antibodies against Shiga-like toxin from *Escherichia coli*. Infect. Immun. *50*, 695–700.

Subtil, A., Gaidarov, I., Kobylarz, K., Lampson, M.A., Keen, J.H., and McGraw, T.E. (1999). Acute cholesterol depletion inhibits clathrin-coated pit budding. Proc. Natl. Acad. Sci. USA *96*, 6775–6780.

Takaoka, A., Mitani, Y., Suemori, H., Sato, M., Yokochi, T., Noguchi, S., Tanaka, N., and Taniguchi, T. (2000). Cross talk between interferon-gamma and -alpha/beta signaling components in caveolar membrane domains. Science *288*, 2357–2360.

Tesh, V.L., Ramegowda, B., and Samuel, J.E. (1994). Purified Shiga-like toxins induce expression of proinflammatory cytokines from murine peritoneal macrophages. Infect. Immun. *62*, 5085–5094.

van Setten, P.A., Monnens, L.A., Verstraten, R.G., van den Heuvel, L.P., and van Hinsbergh, V.W. (1996). Effects of verocytotoxin-1 on nonadherent human monocytes: binding characteristics, protein synthesis, and induction of cytokine release. Blood *88*, 174–183.

Varma, R., and Mayor, S. (1998) GPI-anchored proteins are organized in submicron domains at the cell surface. Nature *394*, 798–801.

Verkade, P., Harder, T., Lafont, F., and Simons, K. (2000). Induction of caveolae in the apical plasma membrane of Madin-Darby canine kidney cells. J. Cell Biol. *148*, 727–739.

Wesche, J., Rapak, A., and Olsnes, S. (1999). Dependence of ricin toxicity on translocation of the toxin A-chain from the endoplasmic reticulum to the cytosol. J. Biol. Chem. *274*, 34443–34449.

White, J., Johannes, L., Mallard, F., Girod, A., Grill, S., Reinsch, S., Keller, P., Echard, A., Goud, B., and Stelzer, E.H.K. (1999) Rab6 coordinates a novel Golgi to ER retrograde transport pathway in live cells. J. Cell Biol. *147*, 743–759.

Zoon, K.C., Arnheiter, H., Zur Nedden, D., Fitzgerald, D.J. and Willingham, M.C. (1983) Human interferon alpha enters cells by receptor-mediated endocytosis. Virology *130*, 195–203.